Experimental testing in 3-point bending of sandwich beams using additively manufactured loading bars

Andrei NENCIU*,[1,2], Dragos Alexandru APOSTOL[2],
Dan Mihai CONSTANTINESCU[2]

*Corresponding author
*,[1]INCAS – National Institute for Aerospace Research "Elie Carafoli",
B-dul Iuliu Maniu 220, Bucharest 061136, Romania,
nenciu.andrei@incas.ro
[2]Department of Strength of Materials,
National University of Science and Technology POLITEHNICA Bucharest,
Splaiul Independentei 313, 060042, Bucharest, Romania,
dragos.apostol@upb.ro, dan.constantinescu@upb.ro

DOI: 10.13111/2066-8201.2025.17.1.4

Received: 07 February 2025/ Accepted: 20 February 2025/ Published: March 2025

Abstract: *This study investigates the feasibility of custom-made 3D-printed loading bars of a testing machine and compares their performance to that of standard (metal) components through the 3-point bending testing of sandwich beams. Specifically, the study evaluates two types of sandwich beams: honeycomb and re-entrant unit cell topologies. Each type of beam was subjected to three-point bending tests using both standard and 3D-printed loading bars. The experiments indicate that the printed custom-made loading bars used as a testing accessory are a viable alternative. Further research with a larger number of samples is needed to address the potential of generating a possible defect during the printing process and its propagation during testing.*

Key Words: *additive manufacturing, sandwich structures, honeycomb, re-entrant, 3D-printing, 3-point bending*

1. INTRODUCTION

As manufacturing technologies have advanced, sandwich panels have emerged as a technically viable alternative to conventional structures, providing superior properties and performance across a range of loading conditions relative to production costs. This has led to their widespread adoption, particularly in the aerospace industry, [1]-[3], as well as in other fields, [4], [5]. At the same time, the 3-point bending loading of beams, [6], [7], is a study of interest for obtaining the core behaviour of beams, [8]-[10], or even for testing different types of materials, [11]. These studies are necessary for understanding the behaviour of sandwich beams and panels of various topologies. Moreover, another trend that has gained momentum in recent years and continues to grow is 3D printing, [12].
Given these considerations, the following research avenue can be explored: the production of testing machine accessories by additive manufacturing for standardized testing. If these components are properly designed, they could avoid negatively impacting results or

compromising study integrity. The ability to create custom testing accessories could open new research possibilities, provided that comparative studies show that tests conducted with 3D-printed components yield results consistent with those obtained using approved, standardized metal-made equipment. Therefore, a comparative study is crucial to determine if 3D-printed accessories can introduce any local effects on test results and whether this new research direction deserves further investigation.

2. GEOMETRY PREPARATION

In order to carry out this comparative study, it was first necessary to identify the appropriate test for which the 3D printed parts would be manufactured, as well as selecting the type of parts to be tested. Given the focus on 3D printing, the most effective approach for this comparative analysis would involve components produced through additive manufacturing. Furthermore, to assess whether there is a correlation between the performance of testing accessories with standard parts and those produced by 3D printing, a study on the behaviour of two types of sandwich beams was conducted.

Specifically, the focus was directed towards the classic honeycomb structure and the increasingly studied re-entrant topology. The objective is to test these two geometries and determine if there is a correlation between the results of each individually tested beam, as well as the differences in results between the two geometries. To ensure that the test results are interpretable, the most appropriate method for evaluating these geometries is through three-point bending tests. This approach will allow for the identification of potential failures, particularly those arising from defects introduced during the 3D printing process.

To fabricate the two types of beams, it was first necessary to identify a common element geometry of each topology, [13]. In order to observe the behaviour of the sandwich beams, the classical three-point bending test was performed. We considered the same relative density, which led to the final configurations, as shown in Figure 1. These dimensions were selected based on an analysis of the test capabilities of the mechanical testing system Zwick Roell Z010, with a maximum force of 10 kN. The beams, each with a length of 70 mm, were tested in accordance with ASTM C393, [14]. The distance between the two supporting loading bars was set at 50 mm, allowing 10 mm of the beam to extend beyond the supports on each side during the test. The beams have a width of 10 mm and a total height of 19.32 mm, including their two face sheets (skins); it should be mentioned that this is a non-standard configuration.

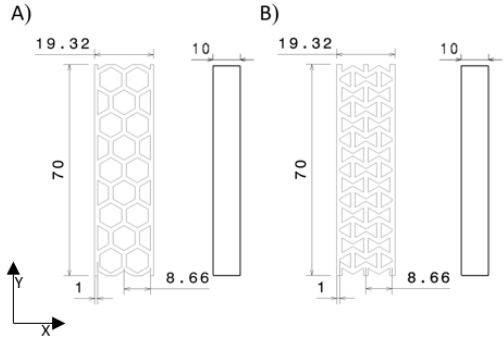

Figure 1. Dimensions of A) Honeycomb beam and B) Re-entrant beam

Once the beams were fabricated, the test accessories to be 3D printed were selected by observing the load configuration and based on the test results. Thus, as shown in Figure 2,

only the loading bars appear to be the only elements that need to be 3D printed. This conclusion is evident, as the local crushing effects will not extend beyond this area.

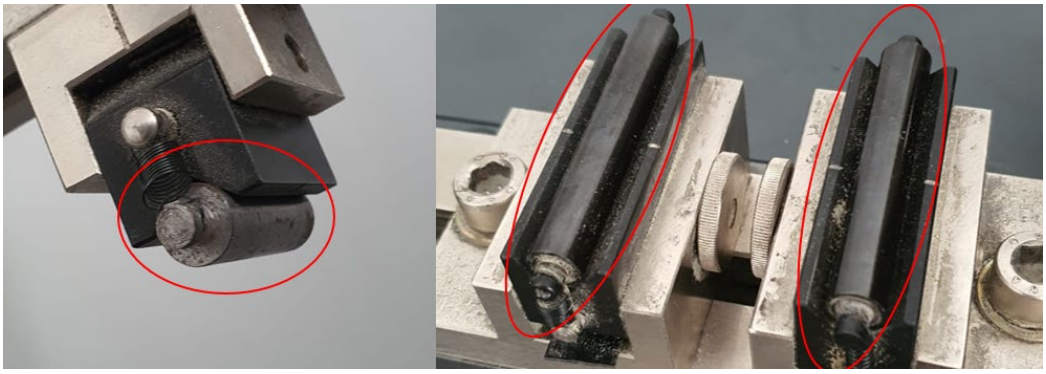

Figure 2. The upper and the two lower loading bars chosen for 3D printing

Subsequently, based on the measurements of these loading bars, an equivalent design suitable for 3D printing was done.

The next step involves fabricating the beams and the loading bars utilizing the previously developed design parts.

The printing procedure proceeded without any issues as both the loading bars and beams were produced without complications. This process used a Fused Deposition Modelling (FDM) printer which utilized Polylactic Acid (PLA), [15] as material.

The parts, printed on an Ender 3, [16] and sliced using Prusa, [17] were configured for high quality and maximum strength, with a layer height of 0.2 mm and 100% infill.

Three solid layers are used top and bottom, with 2 minimum perimeters. Extrusion width varies between 0.4 mm and 0.6 mm, optimized for different areas. Skirting option is enabled, but brim option is disabled.

These settings prioritize precision, durability, and a higher quality surface, but with a longer print time.

Ultimately, a total of sixteen beams were produced – eight honeycomb and eight re-entrant – as well as three loading bars, one shorter for upper loading and two longer for the lower supports, as to be seen in Figure 3.

Figure 3. Loading bars from standard (S) and 3D printed (P) PLA material

3. TEST RESULTS

As outlined in the first chapter, the objective of this research is to examine and compare if there are any difference between experiments performed with metal and with 3D-printed components.

This comparison is considered essential because not all researchers have access to the necessary resources for conducting the desired tests. Thus, this approach may provide a viable alternative for those with limited resources.

Thus, the 16 beams were categorized into two groups: those tested with standard (S) metal components and those tested with 3D-printed (P) components, with each group consisting of 4 honeycomb (HC) beams and 4 re-entrant (RE) beams. This approach allows for an evaluation of both the differences between the two testing methods and the variations between the two configurations. Thus, it will be done an assessment of whether the use of custom-manufactured accessories is a viable alternative.

Initial tests were conducted using standard components for both honeycomb and re-entrant beams. The results for each beam type were consistent, presenting similar values and behaviour throughout the testing and failure phases.

Figure 4 and Figure 8 illustrate the honeycomb, and re-entrant beams before and after the test, with a more severe failure of the re-entrant beams evident from the fragmentation observed.

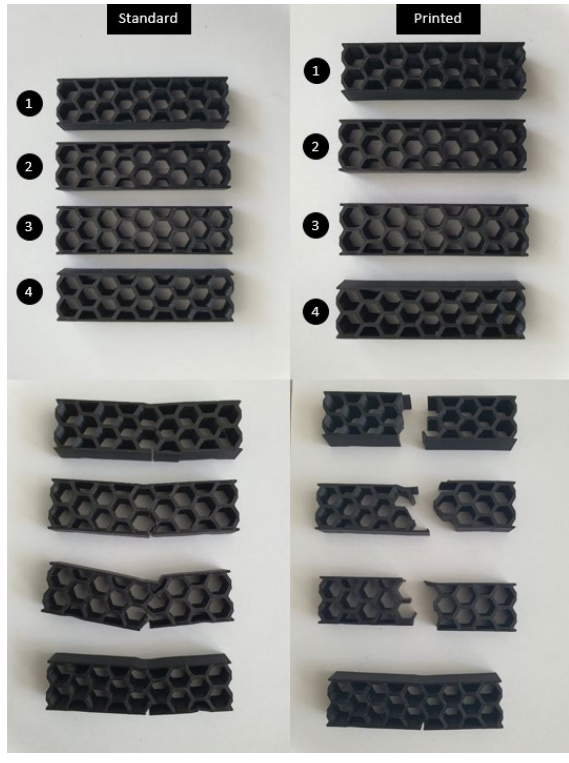

Figure 4. Honeycomb (HC) beams before and after being tested with standard (S) and 3D-printed (P) loading bars

For the first group, an analysis of the actual force values and maximum displacements for the beams reveals only minimal differences between the two specimen types, as well as notable uniformity among beams of the same type.

The graphs presented below, display the force-displacement curves for each individual beam, four of each type: (S) and (P).

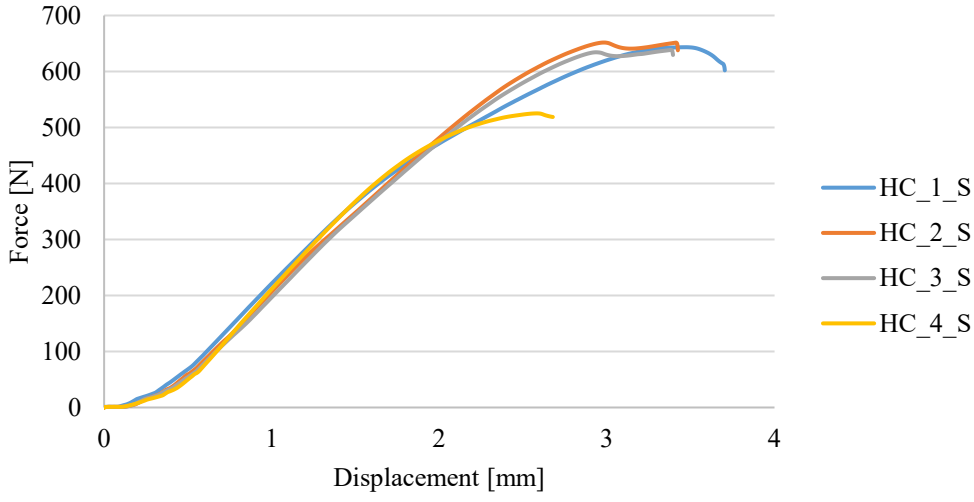

Figure 5. Honeycomb beams tested with standard material (S) loading bars

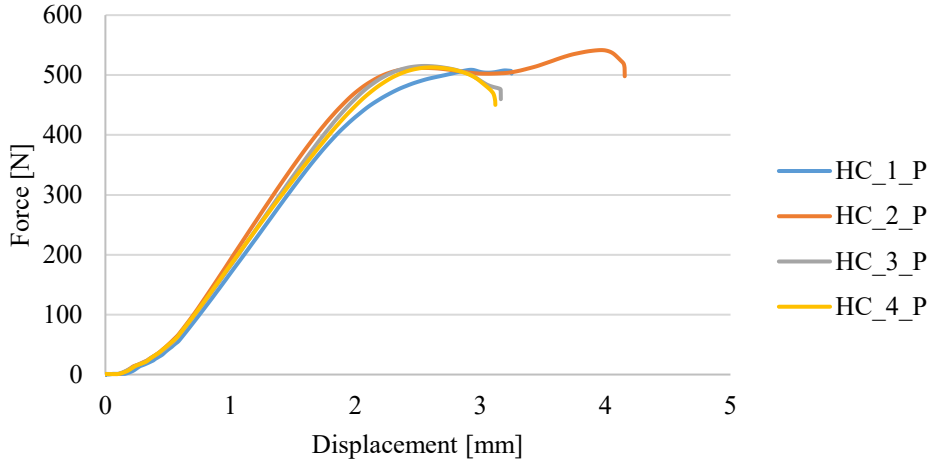

Figure 6. Honeycomb beams tested with 3D-printed material (P) loading bars

After finishing the first set of tests, the standard loading bars were replaced with the 3D-printed ones, see Figure 7, and tests started on the second group of beams.

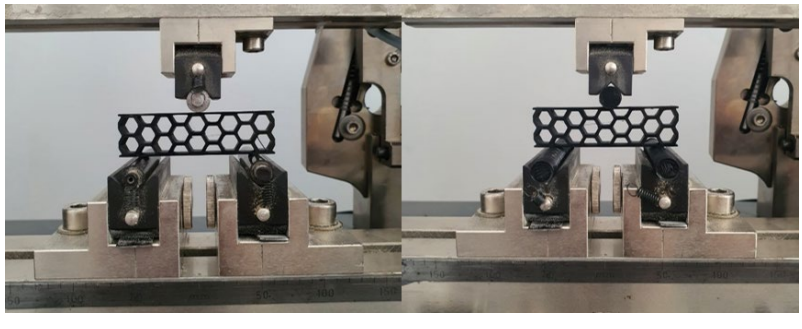

Figure 7. Standard material (S) loading bars (left) and 3D-printed material (P) (right)

The mechanical behaviour of the second group beams tested with the 3D-printed loading bars was slightly different from that of the beams tested with the standard ones. The honeycomb beams tested using standard anvils show a uniform behaviour, as it can be seen in Figure 5, having an average force at failure of 614.74 N.
This value considers the beam that failed much earlier due to a defect during printing, without it the average value would be 644.58 N. On the other hand, the honeycomb beams tested with printed loading bars (Figure 6) had a slightly different behaviour, reaching an average lower force at failure of 519.56 N.
Although the re-entrant (RE) cell beams presented in Figure 8 generally maintained a similar failure force value in terms of force magnitude, the honeycomb beams failed at a significantly earlier stage compared to those tested with standard loading bars.
Moreover, the failure of the re-entrant beams resulted, generally, in complete sectioning, a failure mode not observed for the honeycomb beams tested with standard loading bars, as shown in Figure 4.

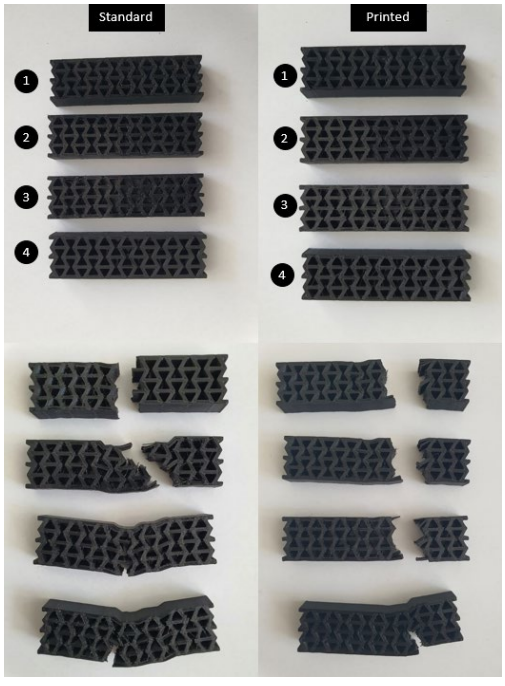

Figure 8. Re-entrant beams before and after being tested with standard (S) and 3D-printed (P) loading bars

The re-entrant beams showed a more uniform failure mode, both in terms of maximum force as well as the shape and surface of failure. At a first glance, it may seem that the loading bars influence significantly the behaviour of the tested beams. However, the potential for defect propagation during the printing process must also be considered. This aspect will be further mentioned in the conclusions.
As it was also observed for the honeycomb tested beams, there is a uniformity in the way the re-entrant beams behaved during the test.
In Figure 9, the standard (S) anvils behaved similarly throughout, having an average force value at failure of 538.39 N.
While, in Figure 10, a similar behaviour is seen for the beams tested with printed (P) anvils, and excluding one of the beams that failed prematurely (RE_P_4), the average force at failure being 578.46 N. By considering all the tests the average force at failure is 561.18 N.

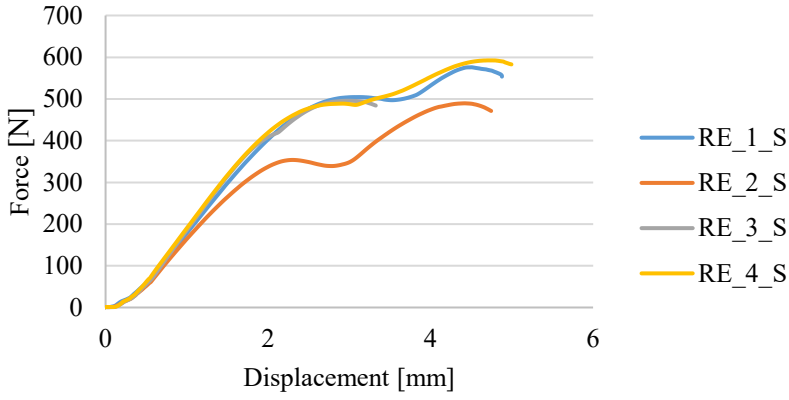

Figure 9. Re-entrant beam tested with standard material (S) loading bars

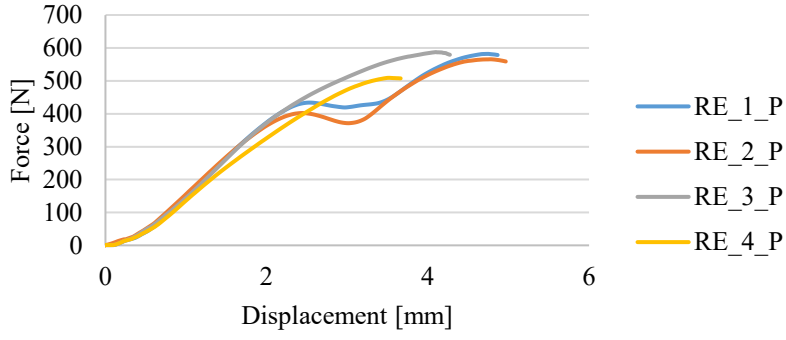

Figure 10. Re-entrant beam tested with 3D-printed material (P) loading bars

With all the test results available, the behaviour of the beams can now be evaluated and analysed, allowing us to draw conclusions regarding the viability and reliability of using the printed anvils in these tests. Once the results of both test methods have been extracted, the results can be compared between the two methods. As can be seen in Figure 11, for the honeycomb beams there is a notable difference in the value of the force at failure between the two test methods, but the displacement at which failure is produced remains the same. On the other hand, when analysing Figure 12, we can see that the behaviour of the beams is about the same, the re-entrant topology presenting a quite similar behaviour for both roller materials.

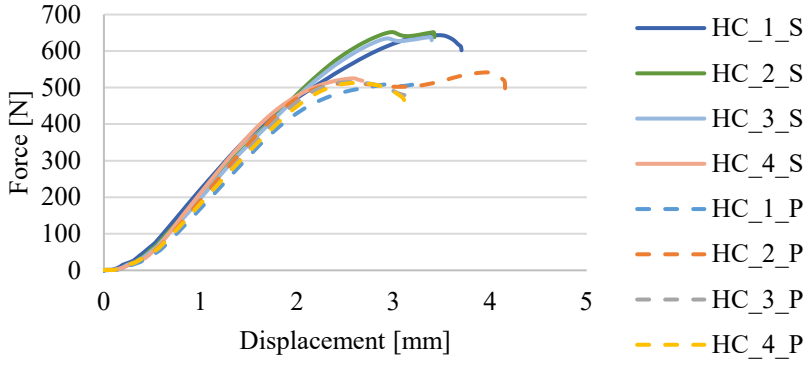

Figure 11. Honeycomb beams tested with standard (S) vs. 3D-printed material (P) loading bars

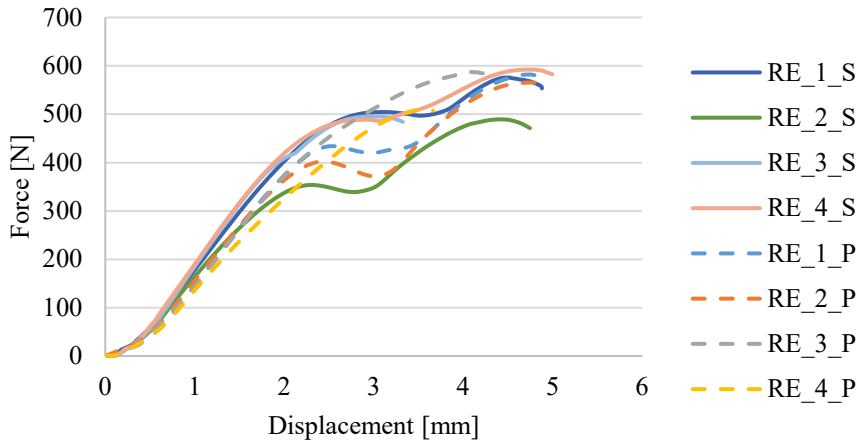

Figure 12. Re-entrant beams tested with standard (S) vs. 3D-printed material (P) loading bars

Thus, by extracting from the graphs presented above the values of the forces at failure and the corresponding displacement, the beams can be analysed individually. In Table 1, data can be observed for all the tested beams. The difference, which is easy to observe, is due, at least in the case of honeycomb beams, to the notable variation in the force at failure. Yet, from an error point of view, based on beams behaviour, this can be attributed to possible defects which resulted during the printing process.

Table 1. Summary of three-point bending test results

Beam	Loading bars	Force [N]	d [mm]
HC 1	Standard	643.42	3.70
HC 2		651.76	3.42
HC 3		638.56	3.39
HC 4		525.25	2.67
Mean Value		*614.75*	*3.29*
HC 1	Printed	508.72	3.24
HC 2		541.62	4.15
HC 3		515.17	3.16
HC 4		512.75	3.11
Mean Value		*519.56*	*3.41*
RE 1	Standard	575.93	4.87
RE 2		489.53	4.74
RE 3		495.65	3.32
RE 4		592.44	4.99
Mean Value		*538.39*	*4.48*
RE 1	Printed	582.12	4.86
RE 2		565.76	4.96
RE 3		587.50	4.27
RE 4		509.36	3.66
Mean Value		*561.18*	*4.44*

Based on data cross-reference, the possibility of using 3D printed parts for testing is an option to be considered if the standards and working methodology are respected.

5. CONCLUSIONS

Upon conducting a comprehensive analysis of the beams, two distinct patterns of behaviour emerged.

Firstly, when evaluating all beams, it became evident that the standard or printed loading bars did not infringe any significant influence on the local effects that might compromise the results. However, a substantial variation was observed between the values of the honeycomb beams from the first and second group, but this is attributed to possible defects which may have resulted during the printing of the beams.

Secondly, the deformation of the beams did not appear to be impacted by the presence of standard or printed loading bars, indicating that the printed ones did not influence the behaviour of the beams in any uncommon way. Notably, a significant difference was observed between the first and second group of beams, the second failing by complete rupture in most cases.

Finally, the substantial discrepancy in the strength values of the honeycomb beams has its origins from geometric defects induced by 3D printing. If the variation were due to any other factors, it would have been evident in both cases rather than being isolated to one set of beams. Unfortunately, the limited number of tested beams was insufficient to conclusively eliminate the potential effects of the printing defects.

When comparing all the beams based on the data presented in the graphs, it is evident that the most significant deviation in the maximum force, of 16.78%, occurs between the honeycomb beams tested with standard and with 3D-printed loading bars. In contrast, the difference between the re-entrant topology beams tested with standard loading bars and those 3D-printed is noticeably lower, at 4.15%.

Furthermore, the relative error in maximum force test results between beams from the first group, which were tested using standard anvils, and those from the second group tested with 3D-printed anvils, ranged from 13.24% to 7.70%, resulting in a deviation of only 5.54%.

Table 2. Relative error of maximum force test results

	HC_S [%]	**HC_P [%]**	**RE_S [%]**	**RE_P [%]**
HC_S	-	16.78	13.24	9.11
HC_P	16.78	-	3.56	7.70
RE_S	13.24	3.56	-	4.15
RE_P	9.11	7.70	4.15	-

From the study presented, it can be concluded that the use of 3D-printed components does not introduce a high degree of error or uncertainty for conventional mechanical testing. However, it is important to note that future studies should include a larger sample size to address potential defects associated with the 3D printing of sandwich beams and components.

REFERENCES

[1] B. Castanie, C. Bouvet, M. Ginot, Review of composite sandwich structure in aeronautic applications, *Composites Part C: Open Access*, Volume **1**, 100004, 2020.

[2] A. Krzyzak, M. Mazur, M. Gajewski, K. Drozd, A. Komorek, P. Przybyłek, Sandwich Structured Composites for Aeronautics: Methods of Manufacturing Affecting Some Mechanical Properties, *International Journal of Aerospace Engineering*, Volume **2016**, 7816912, 2016.

[3] A. Stefan, G. Pelin, C.-E. Pelin, A.-R. Petre, M. Marin, Manufacturing process, mechanical behavior and modeling of composites structures sandwich panel, *INCAS BULLETIN*, Volume **13**, issue 1, 183-191, 2021.

[4] A. Pavlović, D. Sintoni, G. Minak, C. Fragassa, On the modal behaviour of ultralight composite sandwich automotive panels, *Composite Structures*, Volume **248**, 112523, 2020.
[5] Y. Garbatov, S. Scattareggia Marchese, G. Epasto. V. Crupi, Flexural response of additive-manufactured honeycomb sandwiches for marine structural applications, *Ocean Engineering*, Volume **302**, 117732, 2024.
[6] Z. Jin, W. Mao, F. Yang, Failure analysis of sandwich beams under three-point bending based on theoretical and numerical models, *Science and Engineering of Composite Materials*, Volume **30**, 20220224, 2023.
[7] H. Yuan, J. Zhang, H. Sun, The failure behavior of double-layer metal foam sandwich beams under three-point bending, *Thin-Walled Structures*, Volume **80**, 109801, 2022.
[8] J. Arbaoui, Y. Schmitt, J-L Pierrot, F-X. Royer, Effect of Core Thickness and Intermediate Layers on Mechanical Properties of Polypropylene Honeycomb Multi-Layer Sandwich Structures, *Archives of Metallurgy and Materials*, Volume **59**, 2014.
[9] H. Qiang, L. Lizheng, J Xuwen, J. Yonggang, Y. Dejun, Study on three-point bending behavior of sandwich beams with novel auxetic honeycomb core, *Materials Today Communications*, Volume **35**, 106259, 2023.
[10] F. Xia, Y. Durandet, P.J. Tan, D. Ruan, Three-point bending performance of sandwich panels with various types of cores, *Thin-Walled Structures*, Volume **179**, 109723, 2022.
[11] H. Balcıoğlu, Flexural Behaviors of Sandwich Composites Produced Using Recycled and Natural Material, *Mugla Journal of Science and Technology*, Volume **4**, 64-73, 2018.
[12] X. Tian, A. Todoroki, T. Liu, L. Wu, Z. Hou, M. Ueda, Y. Hirano, R. Matsuzaki, K. Mizukam, K. Iizuka, A-V. Malakhoi, A-N. Polilov, D. Li, B. Lu, 3D Printing of Continuous Fiber Reinforced Polymer Composites: Development, Application, and Prospective, *Chinese Journal of Mechanical Engineering: Additive Manufacturing Frontiers*, Volume **1**, 100016, 2022.
[13] Z. Wang, Y. Wang, J. He, K. Dong, G. Zhang, W. Li, Y. Xiong, Additive Manufacturing of Continuous Fiber-Reinforced Polymer Composite Sandwich Structures with Multiscale Cellular Cores, *Chinese Journal of Mechanical Engineering: Additive Manufacturing Frontiers*, Volume **2**, 100088, 2023.
[14] * * * ASTM C393/C93M-20, Standard Test Method for Core Shear Properties of Sandwich Constructions by Beam Flexure, *ASTM International*, West Conshohocken. PA. USA, 2020.
[15] J. Prusa, *Technical datasheet Prusament PLA by Prusa Polymers*, February 2022, https://prusament.com/wp-content/uploads/2022/10/PLA_Prusament_TDS_2021_10_EN.pdf, accessed in July 2024.
[16] Creality. (n.d.). *Ender 3 3D Printer*. Retrieved from https://www.creality.com/products/ender-3-3d-printer?cfb=51816b7e-532b-4dc6-a084-c59922667fbf&ifb=51816b7e-532b-4dc6-a084-c59922667fbf&scm=search.v39.101.768.103.104&score=1&ssp=&spm=..index.header_1.1 accessed in July 2024.
[17] Prusa Research, *PrusaSlicer: Open-source slicing software for 3D printing*, Prusa Research, 2024. [Online]. Available: https://www.prusa3d.com/prusaslicer/ accessed in July 2024.